AGU PUBLICATIONS

Geophysical Research Letters

RESEARCH LETTER
10.1002/2015GL065248

Special Section:
First Results from the MAVEN Mission to Mars

Magnetotail dynamics at Mars: Initial MAVEN observations

Gina A. DiBraccio[1], Jared. R. Espley[1], Jacob R. Gruesbeck[1,2], John E. P. Connerney[1], David A. Brain[3], Jasper S. Halekas[4], David L. Mitchell[5], James P. McFadden[5], Yuki Harada[5], Roberto Livi[5], Glyn Collinson[1,6], Takuya Hara[5], Christian Mazelle[7,8], and Bruce M. Jakosky[3]

[1]Solar System Exploration Division, NASA Goddard Space Flight Center, Greenbelt, Maryland, USA, [2]Department of Astronomy, University of Maryland, College Park, Maryland, USA, [3]Laboratory for Atmospheric and Space Physics, University of Colorado Boulder, Boulder, Colorado, USA, [4]Department of Physics and Astronomy, University of Iowa, Iowa City, Iowa, USA, [5]Space Sciences Laboratory, University of California, Berkeley, California, USA, [6]Institute for Astrophysics and Computational Sciences, Catholic University of America, Washington, District of Columbia, USA, [7]CNRS, Institut de Recherche en Astrophysique et Planétologie, Toulouse, France, [8]Paul Sabatier University, Toulouse, France

Key Points:
- Initial MAVEN observations demonstrate dynamics of the complex Martian magnetotail
- Observed substorm-like loading/unloading of magnetic flux with signatures of magnetic reconnection
- Escaping high-energy planetary ions are observed exclusively in tail current sheet

Correspondence to:
G. A. DiBraccio,
gina.a.dibraccio@nasa.gov

Citation:
DiBraccio, G. A., et al. (2015), Magnetotail dynamics at Mars: Initial MAVEN observations, *Geophys. Res. Lett.*, *42*, doi:10.1002/2015GL065248.

Received 6 JUL 2015
Accepted 3 SEP 2015

Abstract We report on the complex nature of the induced Martian magnetotail using simultaneous magnetic field and plasma measurements from the Mars Atmosphere and Volatile EvolutioN (MAVEN) spacecraft. Two case studies are analyzed from which we identify (1) repetitive loading and unloading of tail magnetic flux as the field magnitude changes dramatically, exhibiting signatures similar to substorm activity within intrinsic magnetospheres; (2) multiple current sheet crossings indicative of plasma sheet flapping; (3) tailward flowing high-energy planetary ions (O^+ and O_2^+), confined exclusively to the cross-tail current sheet, contributing to atmospheric escape; and (4) signatures of magnetic flux ropes, suggesting the occurrence of tail reconnection. These events illustrate the complexity of the Martian magnetotail as MAVEN provides key observations relevant to the unanswered questions of induced magnetosphere dynamics.

1. Introduction

The induced magnetosphere of Mars forms as a result of the interplanetary magnetic field (IMF) draping around the planet's electrically conducting ionosphere [*Spreiter et al.*, 1970; *Nagy et al.*, 2004]. Although Mars lacks an intrinsic magnetic field powered by an active dynamo, it retains localized crustal magnetic fields [*Acuña et al.*, 1998], which add to the complexity of the system. The Martian magnetotail forms as the mass-loaded IMF, a consequence of the extended hydrogen/oxygen corona, becomes draped and elongated behind the planet, due to the solar wind pressure [*Fedorov et al.*, 2006]. The induced magnetotail consists of two lobes, directed sunward and antisunward, separated by a cross-tail current sheet. Unlike an intrinsic magnetotail, the induced tail is particularly active as its structure becomes reoriented in response to variations in IMF direction. This constant reorganization results in an extremely dynamic environment because the orientation and strength of the magnetotail field is highly variable [*Luhmann et al.*, 1991].

Despite their different formation mechanisms, the magnetotails of induced and intrinsic planets are found to have similar processes occurring. At Mars, these similarities include, but are not limited to, the occurrence of magnetic reconnection [*Halekas et al.*, 2009] that can result in the formation of magnetic flux ropes (also known as secondary magnetic islands) [*Eastwood et al.*, 2008]; outflow of low-energy ionospheric ions, lost to the solar wind through the tail lobes, which is likely a major contributor to atmospheric escape [*Kallio et al.*, 1995a, 1995b; *André and Cully*, 2012]; and flapping motions of the tail plasma sheet with associated bursty plasma flows [*Dubinin et al.*, 2012].

There are also many differences between the Martian magnetotail and those of intrinsic origin. At Mars, ions are accelerated tailward in the plasma sheet by the $\mathbf{j}\times\mathbf{B}$ force imposed from magnetic stresses caused by the draped IMF that forms the tail (see review by *Dubinin and Fraenz* [2015]). Because this force is strongest at the center of the tail, ion energies are observed to gradually increase near the plasma sheet [*Rosenbauer et al.*, 1989; *Ip*, 1992; *Dubinin et al.*, 1993, 2011]. For this reason, it is possible to characterize three different regions of the induced magnetotail based on their ion outflow energies and the corresponding energization mechanisms: (1) central tail ion beams ($100\,\mathrm{eV} \leq E \leq 6\,\mathrm{keV}$) that have been accelerated tailward in the plasma sheet by the $\mathbf{j}\times\mathbf{B}$ force; (2) low-energy ions ($E < 100\,\mathrm{eV}$) in the tail lobes, which have likely been accelerated by a

combination of the $\mathbf{j} \times \mathbf{B}$ force, polar wind outflow, trans-terminator ionospheric flow, and wave acceleration [*Dubinin et al.*, 2011]; and (3) high-energy pickup ions ($E > 6$ keV) located in the magnetosheath, just outside of the induced magnetosphere, that are energized by solar wind momentum exchange [*Kallio et al.*, 1995a, 1995b; *Lundin and Barabash*, 2004]. This tailward acceleration of ions, and its contribution to atmospheric escape, has been a major topic of interest at Mars [e.g., *Lundin et al.*, 1989, 2007; *Chassefière and Leblanc*, 2004; *Barabash et al.*, 2007; *Lundin*, 2011; *Dubinin et al.*, 2011, 2012].

Now with the Mars Atmosphere and Volatile EvolutioN (MAVEN) mission [*Jakosky et al.*, 2015] we are able to study the induced Martian magnetotail by utilizing measurements from the comprehensive particle and fields package. Here we present two case studies, using data acquired on 13 November 2014 and 5 May 2015, to report on several features of the magnetotail: (1) repetitive loading and unloading of tail magnetic flux, similar to substorm activity at planets with intrinsic magnetospheres; (2) current sheet dynamics, driven by plasma sheet flapping; (3) tailward flowing high-energy planetary ions observed exclusively when MAVEN is traversing the cross-tail current sheet; and (4) magnetic flux ropes, which are suggestive of magnetic reconnection.

2. MAVEN Magnetotail Observations

2.1. Data and Instrumentation

MAVEN was inserted into orbit around Mars on 22 September 2014 and began providing simultaneous particle and magnetic field measurements shortly thereafter. MAVEN eventually settled into a 75° inclination elliptical orbit with a 4.5 h period. Nominal periapsis and apoapsis occur at altitudes of ~150 km and ~6200 km, respectively, with brief "deep-dip" campaigns during which periapsis is reduced to ~125 km.

The Magnetometer (MAG) [*Connerney et al.*, 2015] provides vector magnetic field data at a maximum sampling rate of 32 vectors per second. The Solar Wind Ion Analyzer (SWIA) [*Halekas et al.*, 2013] and Suprathermal and Thermal Ion Composition (STATIC) (J. McFadden et al., The MAVEN Suprathermal and Thermal Ion Composition (STATIC) instrument, submitted to *Space Science Reviews*, 2015) instruments provide ion measurements at cadences up to 4 s. The Solar Wind Electron Analyzer (SWEA) (D. L. Mitchell et al., The MAVEN Solar Wind Electron Analyzer (SWEA), submitted to *Space Science Reviews*, 2015) provides electron distributions as often as once every 2 s.

MAVEN observations are reported in Mars solar orbital (MSO) coordinates, unless otherwise stated: X_{MSO} is directed from the center of the planet toward the Sun, Z_{MSO} is normal to Mars' orbital plane, and Y_{MSO} completes the right-handed system. The reader is referred to the corresponding instrument papers for additional details regarding instrument specifications and capabilities.

2.2. Loading and Unloading of Magnetic Flux

On 13 November 2014, a repetitive enhancement was observed in the magnetic field data as MAVEN traversed the pre-dawn sector of Mars' magnetotail. An overview of SWEA, STATIC, and MAG data during this orbit, along with a portion of MAVEN's trajectory, appears in Figure 1. MAVEN was in an instrument commissioning phase until 16 November 2014; consequently, some instruments were not making measurements on the day reported here.

MAVEN entered the southern magnetotail, crossing the induced magnetospheric boundary (IMB) at ~08:27:24 UTC (vertical dashed line), at a distance of 1.65 R_M (where R_M is the radius of Mars) downtail in the $-X_{MSO}$ direction. We identify the IMB crossing on the basis of a rotation in the magnetic field vector with a concurrent decrease in overall magnetosheath wave activity. Additionally, the SWEA energy spectra transitioned from a shocked magnetosheath electron population with energies between 20 and 50 eV (the <10 eV population is due to spacecraft charging) to the <20 eV electrons observed within the magnetic pileup region (MPR). MAVEN progressed through the southern tail for ~60 min before encountering highly dynamic magnetic fields in the ionosphere near periapsis and then exiting the magnetosphere on the dayside. We note that the crustal field influence was negligible for this particular orbit and the draped IMF was observed to be ~34 nT, which is not unusual at Mars [*Crider et al.*, 2004].

From the time of the IMB crossing until ~09:20 UTC, MAG observations revealed four periods of rapid field enhancements (numbered in Figure 1h), in both B_X and the total field magnitude, $|B|$, up to ~12 nT followed by an immediate decrease to <2 nT. As $|B|$ increased in each event, the field was predominantly in the sunward, or $+X_{MSO}$, direction, characteristic of the heavily draped IMF forming the tail lobes. During the intervals of decreasing magnetic field magnitude ($|B|$ approached 0 nT), the field rotated away from X_{MSO} and enhanced fluctuations were observed in all three magnetic field components. The diminishing field

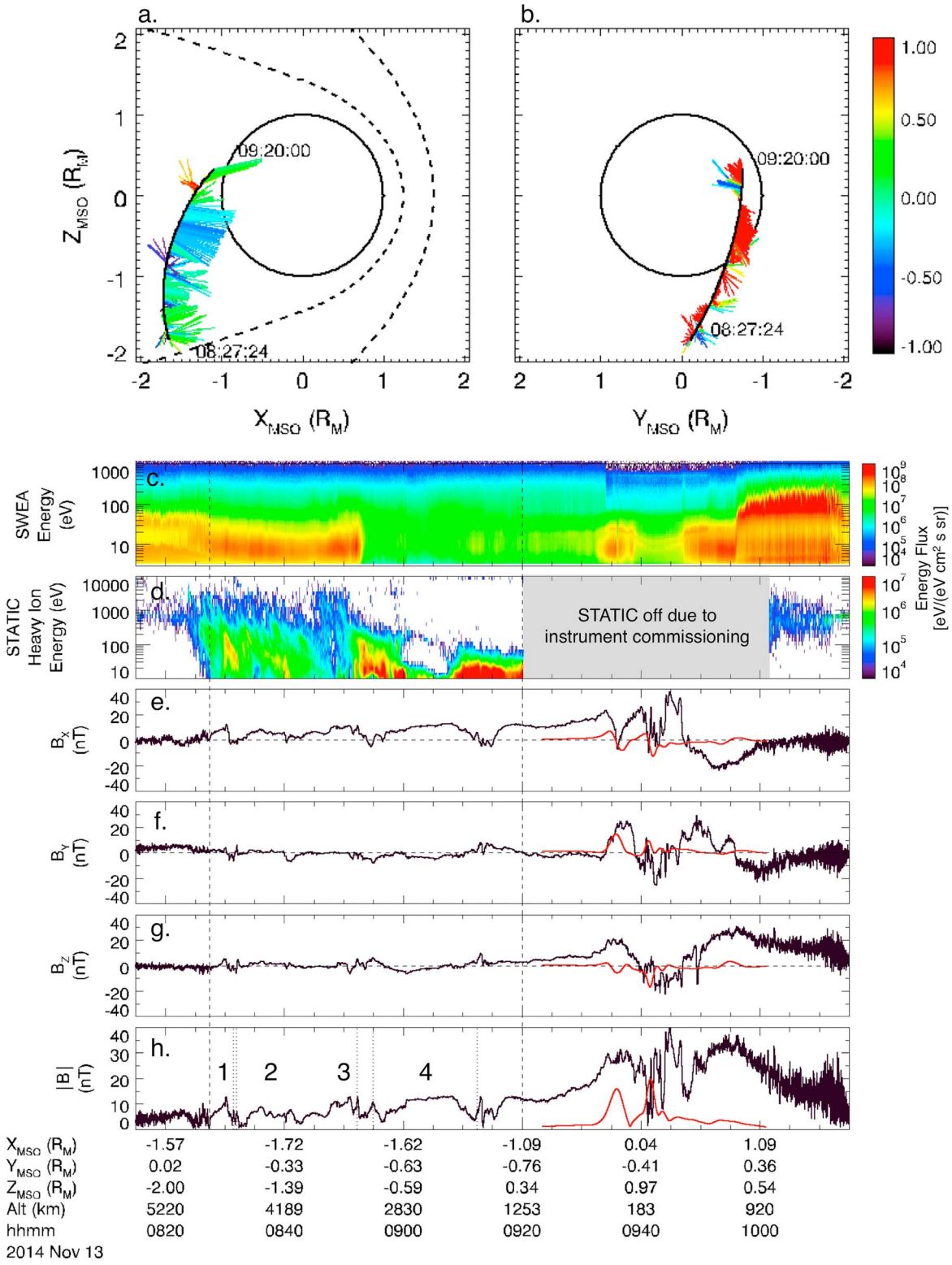

Figure 1. A portion of MAVEN's orbit on 13 November 2014 (corresponding to vertical dashed lines in time series) viewed from (a) the meridional (X_{MSO}–Z_{MSO}) plane and (b) behind the planet toward the Sun (Y_{MSO}–Z_{MSO}). Nominal IMB and bow shock positions [*Trotignon et al.*, 2006] are indicated by dashed lines. Normalized magnetic field vector projections are plotted along the trajectory where the color represents the normalized out-of-plane component: B_Y (Figure 1a) and B_X (Figure 1b). MAVEN plasma and magnetic field data: (c) SWEA electron energy spectra; (d) STATIC energy spectra of heavy ions with $M/q \geq 12$; (e–h) magnetic field components, B_X, B_Y, and B_Z, in MSO coordinates and total field magnitude, $|B|$, provided by MAG (black lines). Red lines in Figures 1e–1h represent crustal magnetic field spherical harmonic model outputs from *Morschhauser et al.* [2014]. In Figure 1h vertical dotted lines mark times that magnetic flux ropes were detected.

magnitude and corresponding rotation from the dominant B_X component to B_Y and B_Z indicate reorganization of the magnetotail. The repetitive increase and decrease of magnetic flux was observed for a period of ~50 min as MAVEN traversed the magnetotail. The location of these four excursions from the draped B_X direction is illustrated in the orbital plot of Figures 1a and 1b.

We attribute this increase-then-decrease of field magnitude to the loading and unloading of tail magnetic flux. Increasing $|B|$ segments, termed "loading," are interpreted as periods when the draped IMF accumulated in the ionosphere, increasing the pileup around Mars and loading the tail with additional magnetic flux. This loading is observed as the rapid enhancements in $|B|$. During this process, the IMF continues to drape around the planet until it is eventually released by one of two mechanisms. In one scenario, field lines gradually slip around the planet and are pulled downtail with the solar wind. In the second scenario, the flux is "unloaded" impulsively as magnetic reconnection occurs within the cross-tail current sheet, detaching large amounts of flux from the tail. Unloading is observed as the sudden decrease in B_X and $|B|$ by a factor of six. Here we find that the loading processes occurred over a span of 3–5 min. The unloading occurred over short intervals of 2–4 min.

This unloading of magnetic flux may be the result of magnetic reconnection, a ubiquitous phenomenon in space plasmas, associated with the changing of magnetic field topology. Close inspection revealed that, during the unloading intervals, fluctuations were present in all three magnetic field components and coincided with momentary increases in $|B|$. Further analysis showed that a bipolar signature in either B_X or B_Z accompanied these localized spikes in $|B|$. This is a characteristic feature of magnetic flux ropes [*Russell and Elphic*, 1979], magnetic structures of helical topology often produced by magnetic reconnection. The vertical dotted lines in Figure 1h identify the times associated with individual flux rope encounters. To confirm their structures, a minimum variance analysis (MVA) [*Sonnerup and Cahill*, 1967] was performed on each individual flux rope (not presented here). The presence of multiple flux ropes throughout the unloading segments supports the hypothesis that magnetic reconnection was likely responsible for the tail magnetic field reconfiguration. However, MAVEN did not encounter the cross-tail current sheet during this particular orbit, making observations of additional signatures associated with reconnection (e.g., plasma jets) unlikely.

Planetary heavy ions were also observed during each of the four unloading periods. Figure 1d shows the STATIC energy spectra for ions with mass-per-charge $(M/q) \geq 12$. Analysis of the three-dimensional energy spectra for these planetary ions reveals that they were flowing tailward, in the $-X_{MSO}$ direction. Additionally, they exhibited energy dispersions similar to the time-dispersed ion signatures reported by *Halekas et al.* [2015], which are thought to be a result of ion pickup in variable electric fields. This outflow of low-energy ionospheric ions may be a major contributor to atmospheric escape at Mars.

Shortly after the IMB crossing (08:29:50 UTC), the first population of cold planetary ions was observed to have energies varying by an order of magnitude, ranging from ~20 to 200 eV, throughout the $|B|$ depression. We observe that the second heavy ion enhancement, around 08:29:56 UT, contains mostly ions with energies of ~20 eV and below. The two subsequent intervals in which heavy ions are observed have a particularly high flux as MAVEN traverses closer to the planet, possibly moving into another acceleration region in the magnetotail. These intervals occurred after the spacecraft passed into the optical shadow behind the planet, which is identified by the transition from the MPR electron spectra to the wake spectra at 08:52:44 UTC. Earlier work using Phobos 2 data concluded that very low energy ($<$100 eV) planetary ions are typically measured within the optical shadow, while those of higher energies are found closer to the IMB [*Kallio et al.*, 1995a, 1995b].

2.3. Cross-Tail Current Sheet Analysis

The draped IMF, forming the Martian magnetotail, creates two lobes of antiparallel field orientation that are separated by a cross-tail current sheet. At Mars, the orientation of this current sheet is constantly changing in response to changes in the IMF direction. Although the magnetic fields in the tail are heavily draped in the $\pm X_{MSO}$ direction, the orientation of the tail and cross-tail current sheet is controlled by the IMF clock angle [*Luhmann et al.*, 1991].

On 5 May 2015, MAVEN's orbital periapsis was located at low latitudes on the dayside. In this configuration, the spacecraft was inside the induced magnetosphere for the duration of the orbit, except for periods of enhanced solar wind pressure, which cause the magnetosphere to compress, pushing the IMB to lower altitudes. As a result, we are unable to measure the upstream IMF orientation. Additionally, MAVEN reached distances of 2.6 R_M downtail in the $-X_{MSO}$ direction, providing some of the most distant magnetotail observations during the mission thus far.

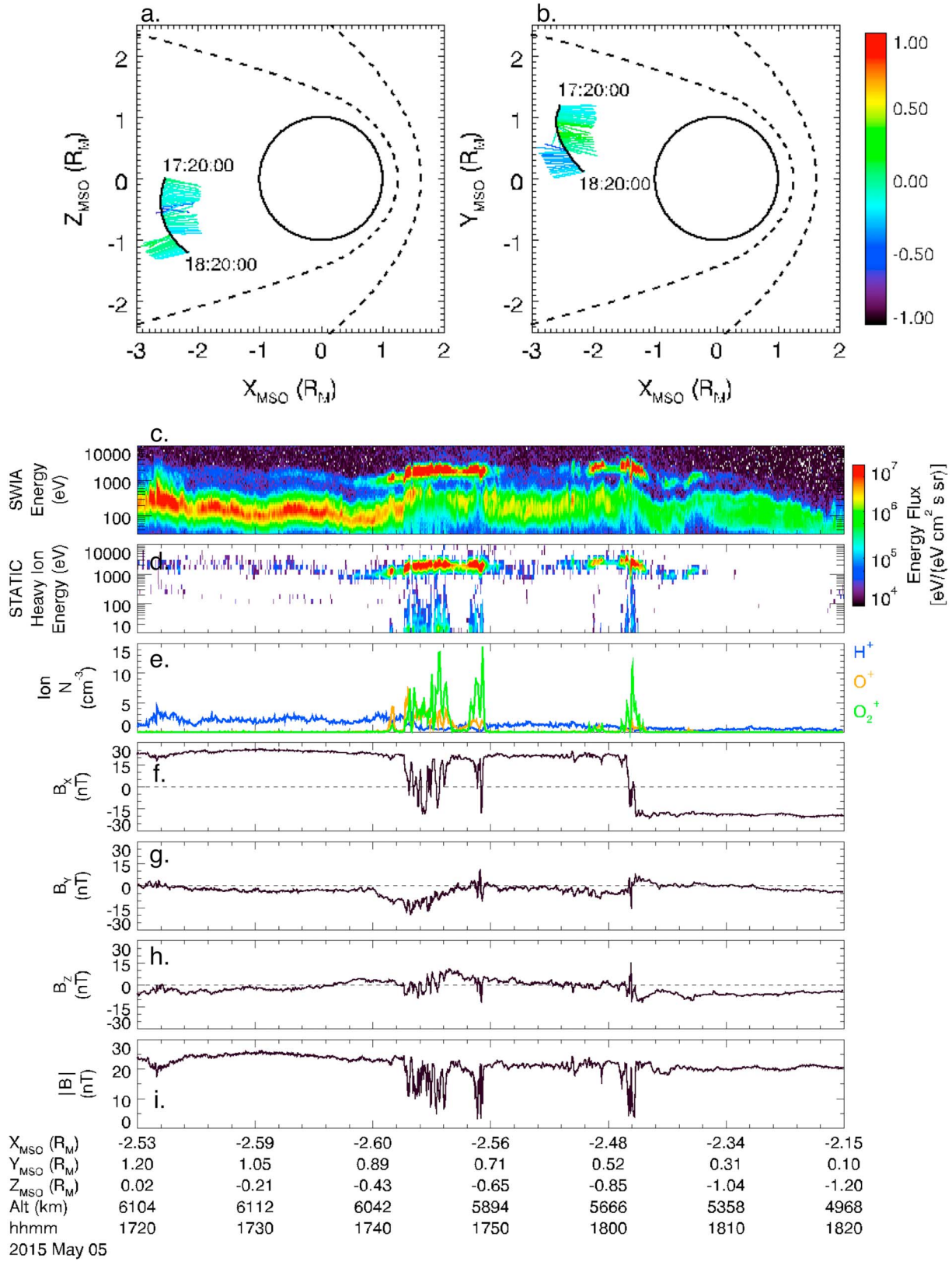

Figure 2. A portion of MAVEN's orbit on 5 May 2015 viewed from the (a) meridional (X_{MSO}–Z_{MSO}) and (b) equatorial (X_{MSO}–Y_{MSO}) planes. See Figure 1 caption. MAVEN plasma and magnetic field data: (c) SWIA ion energy; (d) STATIC energy of heavy ions with $M/q \geq 12$; (e) densities of H^+, O^+, and O_2^+; (f–i) magnetic field components, B_X, B_Y, and B_Z, in MSO coordinates and total field magnitude, $|B|$.

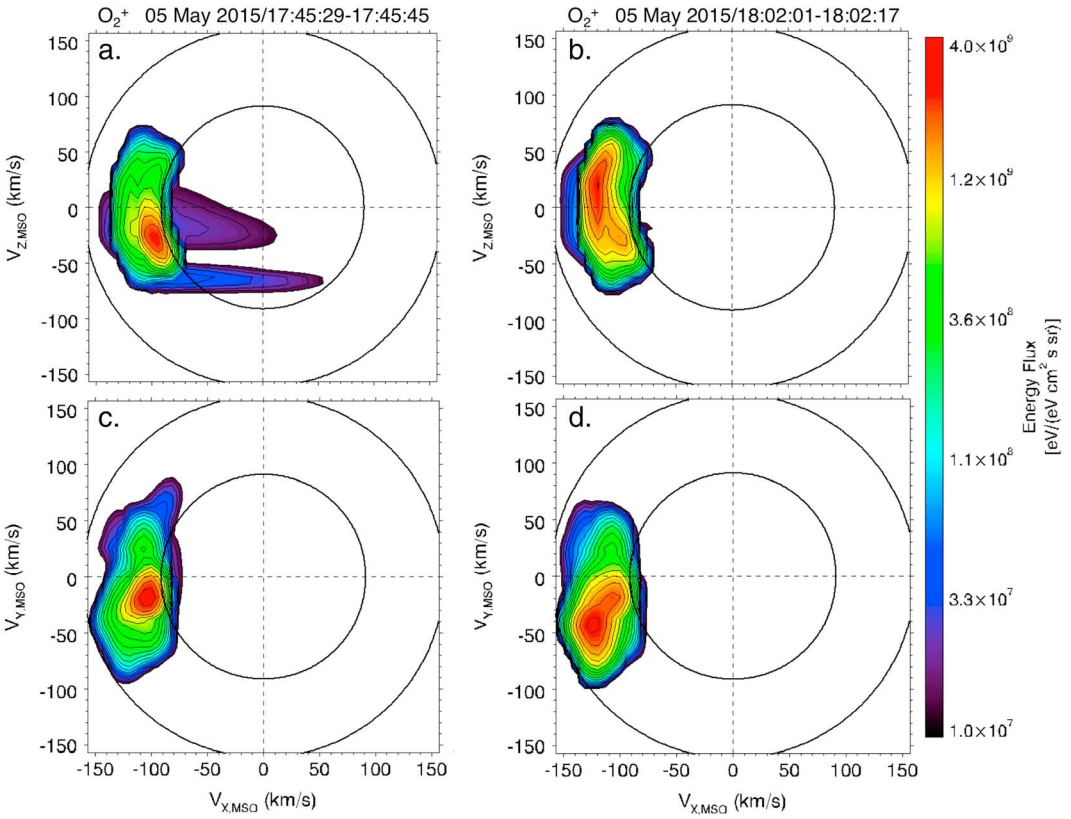

Figure 3. Slices of O_2^+ velocity distribution functions in the (a and b) $V_{X,MSO}$–$V_{Z,MSO}$ and (c and d) $V_{X,MSO}$-$V_{Y,MSO}$ planes for energies between 1–5 keV (concentric circles) during the (Figures 3a and 3c) partial and (Figures 3b and 3d) full current sheet crossings in Figure 2.

Figure 2 shows magnetic field and plasma data, along with a portion of MAVEN's trajectory, as the spacecraft traversed the cross-tail current sheet. The interval begins as MAVEN reached apoapsis, observing a stable and quiet magnetic field, oriented predominantly in the X_{MSO} direction, with a total field magnitude of ~24 nT. A series of 20 partial current sheet crossings are identified in the MAG data, from 17:42:39 UTC to 17:49:27 UTC, by rapid changes in the polarity of $+B_X$, coincident with a decrease in $|B|$. Dramatically enhanced fluctuations are observed in all three components of the field and in $|B|$ as well. These partial crossings were the result of dynamic current sheet flapping, whether steady or kink-like [see *Rong et al.*, 2015a, 2015b]. This flapping may result as the magnetotail responds to varying upstream IMF or from local instabilities propagating along the current sheet. The full current sheet crossing occurred ~11 min later, at 18:01:29 UTC, as B_X changed from +21 nT to −19 nT. During this event, $|B|$ was observed to decrease rapidly from ~23 nT down to ~4 nT over a ~10 s period. A minimum variance analysis revealed that the current sheet normal is oriented mostly in the Y_{MSO} direction, as expected based on typical IMF draping patterns [*Crider et al.*, 2004], with a slight tilt toward Z_{MSO}.

At the time of these current sheet excursions, SWIA measured a high-energy ion population, reaching energies up to 5 keV, confined within the current sheet (Figure 2c). Using the STATIC energy spectra (Figure 2d) of heavy planetary ions ($M/q \geq 12$), we conclude that these high-energy ions are of planetary origin. The planetary ions were enhanced only during current sheet crossings, as evidenced by the densities of H^+, O^+, and O_2^+ displayed in Figure 2e. The density of O_2^+ was ~4 times greater than that of O^+ and an order of magnitude larger than the H^+ ion density. Although slightly higher in energy, these observations are similar to the bursty fluxes of escaping planetary ions reported by *Dubinin et al.* [2012] using Mars Express data.

Ion flow characteristics are illustrated with the help of O_2^+ velocity distribution functions (VDFs) observed during the cross-tail current sheet encounters (displayed in Figure 3 for energies between 1–5 keV).

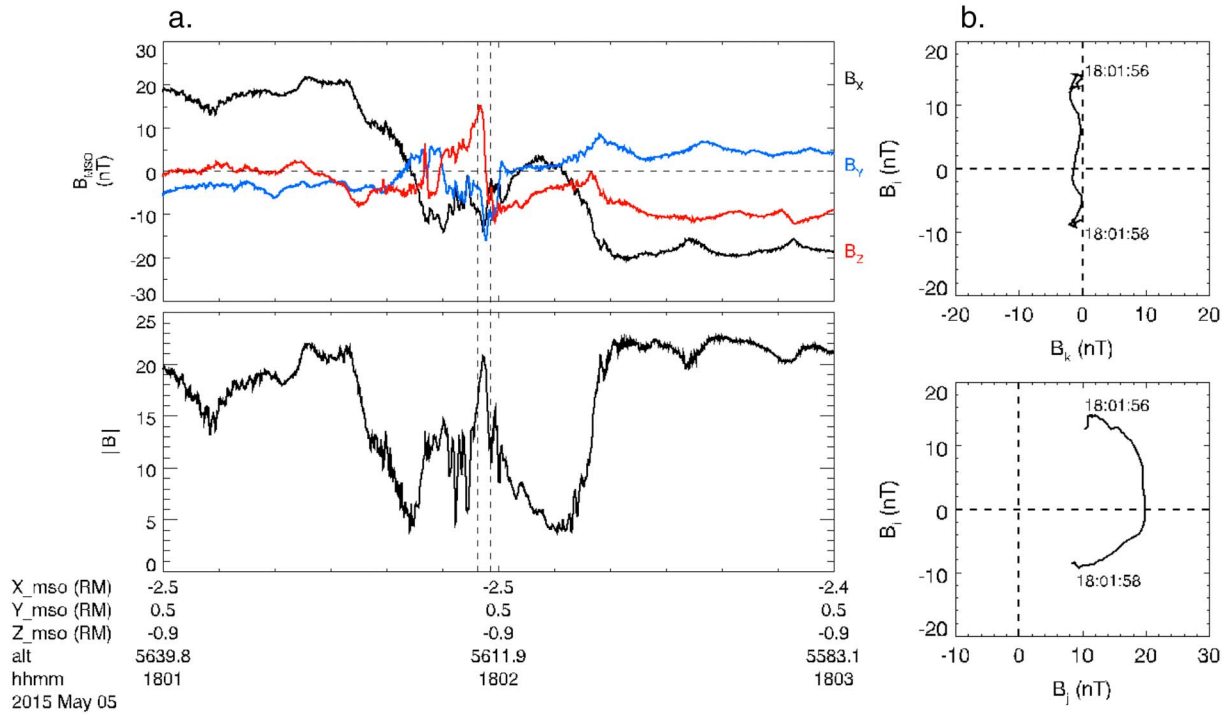

Figure 4. (a) MAG data during the 5 May 2015 current sheet traversal. Vertical dashed lines mark the minimum variance analysis interval. (b) Magnetic field hodograms in minimum variance analysis coordinates.

Figures 3a and 3b show VDFs in the $V_{X,MSO}-V_{Z,MSO}$ plane, while Figures 3c and 3d show VDFs in the $V_{X,MSO}-V_{Y,MSO}$ plane. The O_2^+ VDFs obtained over the interval of partial current sheet crossings (Figures 3a and 3c) are consistent with high-energy ions flowing tailward in the $-V_{X,MSO}$ direction with speeds of ~100 km/s. These O_2^+ ions are also shifted in the $-V_{Y,MSO}$ and $-V_{Z,MSO}$ directions by ~20 km/s and ~30 km/s, respectively. The full current sheet crossing exhibits similar features in the O_2^+ VDFs (Figures 3b and 3d) as the O_2^+ ions moved tailward at speeds >100 km/s with modest contributions in the $-V_{Y,MSO}$ and $+V_{Z,MSO}$ directions. Therefore, we are able to conclude that these escaping planetary ions were traveling downtail along, and within, the cross-tail current sheet.

As suggested by the multiple current sheet crossings, the discontinuity is highly dynamic during this orbit. Figure 4a shows an interval of magnetic field data centered on the full current sheet crossing. This event was not a smooth transition; rather, there were many fluctuations present in all three field components. The main current sheet is defined by the reversal in B_X; however, we identify a second bipolar signature in B_Z from +15 nT to −8 nT near the center of the current sheet at 18:01:56 UTC. This deviation is also coincident with an increase in B_Y and $|B|$ to 16 nT and 20 nT, respectively. This is a classical magnetic flux rope signature. The bipolar B_Z signature is indicative of the helical topology, while the increase in B_Y, and hence $|B|$, indicates the presence of a strong, axial core field.

We performed a MVA over the extent of the flux rope (vertical dashed lines in Figure 4a). The magnetic field vectors have been transformed from MSO into MVA coordinates defined by the minimum (B_k), intermediate (B_j), and maximum variance (B_i) components. The resulting intermediate-to-minimum (λ_j/λ_k) and maximum-to-intermediate (λ_i/λ_j) eigenvalue ratios are 46.0 and 6.31, respectively, demonstrating that the MVA coordinate system is well determined [*Sonnerup and Scheible*, 1998]. The hodograms in Figure 4b show that B_k is relatively constant in the minimum-intermediate (B_k-B_j) plane. Furthermore, a large 180° rotation, indicative of helical flux rope topology, is observed in the maximum-intermediate (B_i-B_j) plane. The presence of this flux rope in the cross-tail current sheet suggests that magnetic reconnection may have occurred between the oppositely oriented fields, energizing plasma in the current sheet.

3. Discussion and Summary

We have reported two case studies to address magnetotail dynamics at Mars, utilizing MAVEN's simultaneous magnetic field and plasma measurements. We report the first observations of loading and unloading of magnetic flux in the Martian magnetotail. Additionally, we observe the tailward escape of planetary ions in association with current sheet crossings and plausible evidence of the occurrence of magnetic reconnection in the induced magnetotail of Mars.

During the tail loading and unloading events, the magnetic field magnitude varied by a factor of ~6 over intervals of 3–5 min. The repetitive characteristics exhibited throughout the unloading periods included changes in field orientation from a strongly draped pattern, predominantly in B_X, to intervals where $|B|$ approached 0 nT with small fluctuations present in B_Y and B_Z. Similar signatures have been observed in the intrinsic magnetotails of Mercury [*Slavin et al.*, 2010, 2012], Earth [e.g., *Baker et al.*, 1996], Jupiter [*Russell et al.*, 2000; *Kronberg et al.*, 2005, 2008], and Saturn [*Jackman et al.*, 2007] and are associated with magnetospheric substorms [*Russell and McPherron*, 1975]. Substorms occur as magnetic energy stored in the tail lobes is rapidly released via magnetic reconnection; this process results in particle energization as well as magnetic field reconfiguration.

During the 13 November 2014 event, the spacecraft did not cross the tail current sheet; rather, it remained inside a single lobe before entering the ionosphere. For this reason, we are unable to directly observe reconnection in the cross-tail current sheet. We infer that reconnection may be responsible for this tail reconfiguration based on repetitive and rapid increase-then-decrease observations in $|B|$, in addition to the presence of magnetic flux ropes. The substorm-like loading and unloading of the tail has implications regarding the removal of flux from the Martian magnetosphere. However, a statistical study is needed to confirm the frequency of such events in order to quantify their impact on the system.

In the second case study, we analyzed an orbit on 5 May 2015 when MAG data revealed a series of partial current sheet crossings followed by a complete current sheet crossing as the spacecraft moved from the sunward- ($+X_{MSO}$) to antisunward-directed ($-X_{MSO}$) tail lobe. The partial crossings, identified by rapid changes in the polarity of B_X, evidenced a direct observation of current sheet flapping. Additionally, the most prominent feature of these crossings were the high-energy (1–5 keV) planetary ions, flowing tailward at speeds of ~100 km/s, identified exclusively during the current sheet encounters, as predicted by *Dubinin et al.* [2012]. Their presence was not detected in the tail lobes.

Earlier Pioneer Venus Orbiter work reported observations of O^+ events accompanied by current sheet crossings in the induced tail of Venus [*Slavin et al.*, 1989], similar to the observations in this analysis. In a study of ion energization and escape in the Martian tail, *Dubinin et al.* [2011] reported that the plasma sheet is formed by ions that have been energized up to several hundreds of eV in the center of the tail. This energization comes from the $\mathbf{j} \times \mathbf{B}$ force resulting from the magnetic shear stress imposed by the draped IMF, which is strongest in the center of the plasma sheet. However, we note that the planetary ions observed by MAVEN are of higher energies (1–5 keV). This suggests that another energization mechanism may be responsible for the energized population. Observations at Earth have found that bursty plasma flows in the magnetotail are associated with tail flapping and may be triggered by magnetic reconnection [*Sergeev et al.*, 2006]. Although bursty plasma flows have been identified in the Martian magnetotail [*Dubinin et al.*, 2012], their association with current sheet flapping motion could not be confirmed, due to the lack of simultaneous plasma and magnetic field measurements.

A magnetic flux rope was identified in the full current sheet crossing. Flux ropes, or secondary magnetic islands, are often by-products of magnetic reconnection. The cross-tail current sheet is an ideal location for this phenomenon to occur, due to the oppositely directed fields in the tail lobes. *Eastwood et al.* [2008] observed a secondary island, along with a characteristic quadrupolar out-of-plane Hall magnetic field signature [see *Sonnerup*, 1979; *Shay et al.*, 1998; *Øieroset et al.*, 2001], indicative of magnetic reconnection, at a low-altitude tail current sheet crossing during the Mars Global Surveyor orbital mapping phase. While Hall fields appear to be commonly identified at Mars [*Halekas et al.*, 2009], we are unable to detect any for this particular current sheet crossing, suggesting that the spacecraft did not pass within close proximity to any reconnection X–lines that might have been present.

These initial MAVEN results illustrate a variety of dynamic phenomena occurring in the Martian magnetotail during these orbits. As MAVEN continues to collect data in the Mars space environment, providing a solid

formation for statistical analyses, with simultaneous magnetic field and plasma data, we may better address outstanding questions. By continuing to probe more deeply into the complex magnetotail of Mars, we will likely enhance our knowledge of both intrinsic and induced magnetotails.

Acknowledgments
The MAVEN project is supported by NASA through the Mars Exploration Program. MAVEN data are publicly available through the Planetary Data System. This research was supported by a NASA Postdoctoral Program appointment at the NASA Goddard Space Flight Center, administered by Oak Ridge Associated Universities through a contract with NASA. Observations with the SWEA instrument were supported by the Centre National d'Etudes Spatiales (CNES).

The Editor thanks Andrei Fedorov and an anonymous reviewer for their assistance in evaluating this paper.

References

Acuña, M. H., et al. (1998), Magnetic field and plasma observations at Mars: Initial results of the Mars global surveyor mission, *Science*, *279*, 1676–1680, doi:10.1126/Science.279.5357.1676.

André, M., and C. M. Cully (2012), Low-energy ions: A previously hidden solar system particle population, *Geophys. Res. Lett.*, *39*, L03101, doi:10.1029/2011GL050242.

Baker, D. N., T. I. Pulkkinen, V. Angelopoulos, W. Baumjohann, and R. L. McPherron (1996), Neutral line model of substorms: Past results and present view, *J. Geophys. Res.*, *101*, 12,975–13,010, doi:10.1029/95JA03753.

Barabash, S., A. Fedorov, R. Lundin, and J.-A. Sauvaud (2007), Martian atmospheric erosion rates, *Science*, *315*, 501–503, doi:10.1126/science.1134358.

Chassefière, E., and F. Leblanc (2004), Mars atmospheric escape and evolution, interaction with the solar wind, *Planet. Space Sci.*, *52*, 1039–1058, doi:10.1016/j.pss.2004.07.002.

Connerney, J. E. P., J. Espley, P. Lawton, S. Murphy, J. Odom, R. Oliversen, and D. Sheppard (2015), The MAVEN magnetic field investigation, *Space Sci. Rev.*, doi:10.1007/s11214-015-0169-4.

Crider, D. H., D. A. Brain, M. H. Acuña, D. Vignes, C. Mazelle, and C. Bertucci (2004), Mars Global Surveyor observations of solar wind magnetic field draping around Mars, *Space Sci. Rev.*, *111*, 203–221, doi:10.1023/B:Spac.0000032714.66124.4e.

Dubinin, E., and M. Fraenz (2015), Magnetotails of Mars and Venus, in *Magnetotails in the Solar System*, edited by A. Keiling, C. M. Jackman, and P. A. Delamere, John Wiley, Hoboken, N. J., doi:10.1002/9781118842324.ch3.

Dubinin, E., R. Lundin, O. Norberg, and N. Pissarenko (1993), Ion acceleration in the Martian tail: Phobos observations, *J. Geophys. Res.*, *98*, 3991–3997, doi:10.1029/92JA02233.

Dubinin, E., M. Fraenz, A. Fedorov, R. Lundin, N. Edberg, F. Duru, and O. Vaisberg (2011), Ion energization and escape on Mars and Venus, *Space Sci. Rev.*, *162*, 137–211, doi:10.1007/S11214-011-9831-7.

Dubinin, E., M. Fraenz, J. Woch, T. L. Zhang, J. Wei, A. Fedorov, S. Barabash, and R. Lundin (2012), Bursty escape fluxes in plasma sheets of Mars and Venus, *Geophys. Res. Lett.*, *39*, L01104, doi:10.1029/2011GL049883.

Eastwood, J. P., D. A. Brain, J. S. Halekas, J. F. Drake, T. D. Phan, M. Øieroset, D. L. Mitchell, R. P. Lin, and M. Acuña (2008), Evidence for collisionless magnetic reconnection at Mars, *Geophys. Res. Lett.*, *35*, L02106, doi:10.1029/2007GL032289.

Fedorov, A., et al. (2006), Structure of the Martian wake, *Icarus*, *182*, 329–336, doi:10.1016/j.icarus.2005.09.021.

Halekas, J. S., J. P. Eastwood, D. A. Brain, T. D. Phan, M. Øieroset, and R. P. Lin (2009), In situ observations of reconnection Hall magnetic fields at Mars: Evidence for ion diffusion region encounters, *J. Geophys. Res.*, *114*, A11204, doi:10.1029/2009JA014544.

Halekas, J. S., E. R. Taylor, G. Dalton, G. Johnson, D. W. Curtis, J. P. McFadden, D. L. Mitchell, R. P. Lin, and B. M. Jakosky (2013), The solar wind ion analyzer for MAVEN, *Space Sci. Rev.*, doi:10.1007/s11214-013-0029-z.

Halekas, J. S., J. P. McFadden, J. E. P. Connerney, J. R. Espley, D. A. Brain, D. L. Mitchell, D. E. Larsen, Y. Harada, T. Hara, and S. Ruhunusiri (2015), Time-dispersed ion signatures observed in the Martian magnetosphere by MAVEN, *Geophys. Res. Lett.*, *42*, doi:10.1002/2015GL064781.

Ip, W. H. (1992), Ion acceleration at the current sheet of the Martian magnetosphere, *Geophys. Res. Lett.*, *19*, 2095–2098, doi:10.1029/92GL02098.

Jackman, C. M., C. T. Russell, D. J. Southwood, C. S. Arridge, N. Achilleos, and M. K. Dougherty (2007), Strong rapid dipolarizations in Saturn's magnetotail: In situ evidence of reconnection, *Geophys. Res. Lett.*, *34*, L11203, doi:10.1029/2007GL029764.

Jakosky, B. M., et al. (2015), The Mars Atmosphere and Volatile Evolution (MAVEN) mission, *Space Sci. Rev.*, doi:10.1007/s11214-015-0139-x.

Kallio, E., H. Koskinen, S. Barabash, R. Lundin, and O. Norberg (1995a), Nightside magnetosheath of Mars: ASPERA observations, *Adv. Space Res.*, *16*(4), 119–122.

Kallio, E., H. Koskinen, S. Barabash, C. M. C. Nairn, and K. Schwingenschuh (1995b), Outflow oxygen in the Martian magnetotail, *Geophys. Res. Lett.*, *22*, 2449–2452, doi:10.1029/95GL02474.

Kronberg, E. A., J. Woch, N. Krupp, A. Lagg, K. K. Khurana, and K.-H. Glassmeier (2005), Mass release at Jupiter: Substorm-like processes in the Jovian magnetotail, *J. Geophys. Res.*, *110*, A03211, doi:10.1029/2004JA010777.

Kronberg, E. A., J. Woch, N. Krupp, A. Lagg, P. W. Daly, and A. Korth (2008), Comparison of periodic substorms at Jupiter and Earth, *J. Geophys. Res.*, *113*, A04212, doi:10.1029/2007JA012880.

Luhmann, J. G., C. T. Russell, K. Schwingenschuh, and Y. Yeroshenko (1991), A comparison of induced magnetotails of planetary bodies: Venus, Mars, and Titan, *J. Geophys. Res.*, *96*, 11,199–11,208, doi:10.1029/91JA00086.

Lundin, R. (2011), Ion acceleration and outflow from Mars and Venus: An overview, *Space Sci. Rev.*, *162*, 309–334, doi:10.1007/s11214-011-9811-y.

Lundin, R., and S. Barabash (2004), The wakes and magnetotails of Mars and Venus, *Adv. Space Res.*, *33*, 1945–1955, doi:10.1016/j.asr.2003.07.054.

Lundin, R., A. Zakharov, R. Pellinen, H. Borg, B. Hultqvist, N. Pissarenko, E. M. Dubinin, S. W. Barabash, I. Liede, and H. Koskinen (1989), First measurements of ionospheric plasma escape from Mars, *Nature*, *341*, 609–612, doi:10.1038/341609a0.

Lundin, R., H. Lammer, and I. Ribas (2007), Planetary magnetic fields and solar forcing: Implications for atmospheric evolution, *Space Sci. Rev.*, *129*, 245–278, doi:10.1007/s11214-007-9176-4.

Morschhauser, A., V. Lesur, and M. Grott (2014), A spherical harmonic model of the lithospheric magnetic field of Mars, *J. Geophys. Res. Planets*, *119*, 1162–1188, doi:10.1002/2013JE004555.

Nagy, A., et al. (2004), The plasma environment of Mars, *Space Sci. Rev.*, *111*, 33–114, doi:10.1023/B:SPAC.0000032718.47512.92.

Øieroset, M., T. D. Phan, M. Fujimoto, R. P. Lin, and R. P. Lepping (2001), In situ detection of collisionless reconnection in the Earth's magnetotail, *Nature*, *412*, 414–417, doi:10.1038/35086520.

Rong, Z. J., S. Barabash, G. Stenberg, Y. Futaana, T. L. Zhang, W. X. Wan, Y. Wei, and X.-D. Wang (2015a), Technique for diagnosing the flapping motion of magnetotail current sheets based on single-point magnetic field analysis, *J. Geophys. Res. Space Physics*, *120*, 3462–3474, doi:10.1002/2014JA020973.

Rong, Z. J., S. Barabash, G. Stenberg, Y. Futaana, T. L. Zhang, W. X. Wan, Y. Wei, X. D. Wang, L. H. Chai, and J. Zhong (2015b), The flapping motion of the Venusian magnetotail: Venus Express observations, *J. Geophys. Res. Space Physics*, *120*, 5593–5602, doi:10.1002/2015JA021317.

Rosenbauer, H., et al. (1989), Ions of Martian origin and plasma sheet in the Martian magnetosphere: Initial results of the TAUS experiment, *Nature*, *341*, 612–614, doi:10.1038/341612a0.

Russell, C. T., and R. C. Elphic (1979), Observations of magnetic flux ropes in the Venus ionosphere, *Nature*, *279*, 616–618, doi:10.1038/279616a0.

Russell, C. T., and R. L. McPherron (1975), The magnetotail and substorms, *Space Sci. Rev.*, *15*, 205–266, doi:10.1007/BF00169321.

Russell, C. T., K. K. Khurana, M. G. Kivelson, and D. E. Huddleston (2000), Substorms at Jupiter: Galileo observations of transient reconnection in the near tail, *Adv. Space Sci.*, *26*, 1499–1504.

Sergeev, V. A., D. A. Sormakov, S. V. Apatenkov, W. Baumjohann, R. Nakamura, A. V. Runov, T. Mukai, and T. Nagai (2006), Survey of large-amplitude flapping motions in the midtail current sheet, *Ann. Geophys.*, *24*, 2015–2024, doi:10.5194/angeo-24-2015-2006.

Shay, M. A., J. F. Drake, R. E. Denton, and D. Biskamp (1998), Structure of the dissipation region during collisionless magnetic reconnection, *J. Geophys. Res.*, *103*, 9165–9176, doi:10.1029/97JA03528.

Slavin, J. A., D. S. Intriligator, and E. J. Smith (1989), Pioneer Venus Orbiter magnetic field and plasma observations in the Venus magnetotail, *J. Geophys. Res.*, *94*, 2383–2398, doi:10.1029/JA094iA03p02383.

Slavin, J. A., et al. (2010), MESSENGER observations of extreme loading and unloading of Mercury's magnetic tail, *Science*, *329*, 665–668, doi:10.1126/Science.1188067.

Slavin, J. A., et al. (2012), MESSENGER and Mariner 10 flyby observations of magnetotail structure and dynamics at Mercury, *J. Geophys. Res.*, *117*, doi:10.1029/2011JA016900.

Sonnerup, B. U. Ö. (1979), Magnetic field reconnection, in *Solar System Plasma Physics*, vol. 3, edited by E. N. Parker, C. F. Kennel, and L. T. Lanzerotti, pp. 47–108, North-Holland, Amsterdam.

Sonnerup, B. U. Ö., and L. J. Cahill Jr. (1967), Magnetopause structure and attitude from Explorer 12 observations, *J. Geophys. Res.*, *72*, 171–183, doi:10.1029/JZ072i001p00171.

Sonnerup, B. U. Ö., and M. Scheible (1998), Minimum and maximum variance analysis, in *Analysis Methods for Multi-Spacecraft Data*, *ISSI Sci. Rep. no. SR-001*, edited by G. Paschmann and P. W. Daly, chap. 8, pp. 185–220, European Space Agency, Noordwijk, Netherlands.

Spreiter, J. R., A. L. Summers, and A. W. Rizzi (1970), Solar wind flow past nonmagnetic planets—Venus and Mars, *Planet. Space Sci.*, *18*, 1281–1299, doi:10.1016/0032-0633(70)90139-X.

Trotignon, J. G., C. Mazelle, C. Bertucci, and M. H. Acuña (2006), Martian shock and magnetic pile-up boundary positions and shapes determined from the Phobos 2 and Mars Global Surveyor data sets, *Planet. Space Sci.*, *54*, 357–369, doi:10.1016/J.Pss.2006.01.003.